A PRESSURE CONTROL SCHEME FOR AIR

BRAKES IN COMMERCIAL VEHICLES

A Thesis

by

CHRISTOPHER LELAND BOWLIN

Submitted to the Office of Graduate Studies of
Texas A&M University
in partial fulfillment of the requirements for the degree of

MASTER OF SCIENCE

December 2005

Major Subject: Mechanical Engineering

A PRESSURE CONTROL SCHEME FOR AIR

BRAKES IN COMMERCIAL VEHICLES

A Thesis

by

CHRISTOPHER LELAND BOWLIN

Submitted to the Office of Graduate Studies of
Texas A&M University
in partial fulfillment of the requirements for the degree of

MASTER OF SCIENCE

Approved by:

Co-Chairs of Committee,	D.V.A.H.G. Swaroop
	K. R. Rajagopal
Committee Member,	John Valasek
Head of Department,	Dennis O'Neal

December 2005

Major Subject: Mechanical Engineering

ABSTRACT

A Pressure Control Scheme for Air Brakes in Commercial Vehicles. (December 2005)

Christopher Leland Bowlin, B.S., Texas A&M University

Co-Chairs of Advisory Committee: Dr. D. V. A. H. G. Swaroop,
Dr. K. R. Rajagopal

This research is focused on developing a control scheme for regulating the pressure in the brake chamber of an air brake system found in most commercial vehicles like trucks, tractor-trailers and buses. Such a control scheme can be used for providing the ground work for future systems such as forward collision avoidance systems, advanced anti-lock brake systems and differential braking systems. The development of this controller involves two tasks. The first task was the development of a control scheme for achieving the desired pressure in the brake chamber. This scheme was based on a mathematical model of the treadle valve of the air brake system. The second task was the implementation of this control scheme on the experimental facility that was set up at Texas A&M University. The results indicate successful control of a desired brake chamber pressure for a demonstrated range of controller gains.

To my mom and dad.

ACKNOWLEDGMENTS

I would like to thank Dr. K. R. Rajagopal and Dr. Darbha Swaroop for accepting me into their research group, sharing their wisdom, and for providing such a great opportunity to learn and grow academically. I would also like to thank Shankar Ram Coimbatore-Subramanian for providing much of the theoretical basis for this project, for his immense help on its success and in documenting our results. I also thank Shankar Vilayannur-Natarajan for his role in this project and Dr. John Valasek for his role on my committee.

I thank Parag, Waqar, Sharat, Anand, and Krishna for maintaining a productive and entertaining office environment. I also extend appreciation to Dr. Bhattacharyya, Dr. Parlos, Dr. Kim, Dr. Hogan, Dr. McDermott, and Dr. Jayasuriya for their guidance through course work and everyday conversations. I thank Dr. Anand, Dr. Lau, Cathy, Kim, Martha, Casey, Amanda, Tabitha, and Gina for all of their help with administrative and advising issues. I thank Mitch, Johnny, Jim and Mike for sharing their technical knowledge and answering my questions thoroughly.

I would especially like to thank Mom, Dad, Grandpa, Andrew, Donnie, Jenn, and big Blake for their love and support as my family. Finally, I thank all of my friends in College Station for their camaraderie and diversions from school and work.

TABLE OF CONTENTS

LIST OF FIGURES

LIST OF TABLES

CHAPTER I

INTRODUCTION

A. Background

This thesis is focused on the development of a model-based control scheme for regulating the air pressure in the brake chamber of the air brake system found in most commercial vehicles like trucks, tractor-trailers and buses. Such a control scheme can be used in advanced Anti-lock Brake Systems (ABS), differential braking systems, and, more immediately, in Adaptive Cruise Control (ACC) systems. A cruise control system is a standard feature in most of the automobiles on the road today. It maintains the vehicle speed to the value set by the driver by automatically adjusting the opening of the engine throttle [1], [2]. A vehicle speed sensor is used to provide the feedback signal to this system. A cruise control system is usually activated by the driver when the vehicle is traveling at medium/high speeds in smoothly flowing traffic. A conventional cruise control system utilizes a Proportional-Integral-Derivative (PID [3]) controller to minimize the error between the desired and the measured vehicle speed [4]. Many modifications have been made to the initial system and adaptive/self-tuning cruise control systems have been developed [4], [5].

Standard cruise controls systems can only be disengaged by the driver through braking or turning a switch. The system has no awareness of road conditions or obstacles on the

_____

This thesis follows the style of *Proceedings of the IEEE*.

roadway. In recent years, studies have been carried out to develop "Adaptive Cruise Control" (ACC) systems or "Autonomous Intelligent Cruise Control" (AICC) systems. Most of these studies have focused on developing such systems for passenger cars. These systems enable a controlled vehicle to maintain a safe following distance by controlling the engine throttle and the brake system in that vehicle. These systems obtain measurements of distance and relative velocity from on-board sensors such as a radar mounted on the vehicle. They are being developed so that they can be engaged in heavy traffic conditions. Studies have been recently carried out to evaluate and implement these systems on vehicles [6]-[8].

ACC systems are primarily a feature of convenience. Their impact on traffic flow stability, congestion, and safety is not clear and is stall an open area of research. Studies in [9] indicate that if the safe following distance is chosen to be a linearly increasing function of vehicle as in systems today, they have a negative influence on traffic flow stability. The choice of safe following distance is a current area of research.

A typical ACC system works in the following way: a high level controller determines the desired acceleration or deceleration of the vehicle based upon sensor readings. Then, a lower level control algorithm determines whether the throttle or the brake needs to be actuated. If it determines that the brakes need to be applied, then the algorithm calculates

the required braking torque. Then the corresponding brake chamber pressure can be achieved by using the control scheme presented in this thesis.

Most tractor-trailer vehicles, large single trucks, and transit, inter-city and school buses are equipped with air brake systems [10]. The air brake system used in commercial vehicles is made up of a pneumatic subsystem and a mechanical subsystem. The pneumatic subsystem includes the compressor, the storage reservoirs, distribution valves, the brake lines, and the foot pedal operated treadle valve. The mechanical subsystem includes the push rod, the slack adjuster, the S-cam, the brake pads and the brake drum. The treadle valve found in typical air brake systems has two circuits – the primary circuit and secondary circuit. When the driver presses the brake pedal, air is metered out from the storage reservoirs to the brake chambers through these two circuits.

There are a number of products that control the flow of pressurized air in a pneumatic system. For most steady state applications, pressure regulation can be achieved by simple mechanical means [11]. However, when a time varying value of pressure is desired, electronic solenoid valves are usually employed. For a typical commercial vehicle, this would require adding a minimum of two electronic solenoid valves; one for each circuit of the treadle valve. Recently, ACC has been implemented on a tractor-trailer by controlling the pressure in the braking system at four independent locations of air supply [12]. The number of solenoids will increase further if it is deemed necessary to control all of the

brake chambers individually. This could be useful for safety applications that require independent brake control of each wheel [13]. Existing ACC systems for commercial vehicles use wheel speed sensors for modulating the pressure in the brake chamber.

The approach followed in this thesis is to regulate the brake chamber pressure using a control scheme based on the model of the treadle valve. This scheme can be used to control the amount of braking required during both normal and emergency brake applications. A model for the pressure transients that relates the brake chamber pressure to the treadle valve plunger displacement and the supply pressure to the treadle valve has been presented in [14]. The controller developed based on this model of the treadle valve regulates the brake chamber pressure by controlling the motion of the treadle valve plunger.

It has been observed from experimental data that a majority of the range of the brake chamber pressure is attained in a very small range of the motion of the treadle valve plunger. This fact coupled with the lack of sensory feedback to the driver, makes it very difficult for a driver to regulate the pressure in the air brake system. Thus, implementing ACC systems on trucks will serve as a feature of convenience, primarily through a reduction in stress on the driver. The scheme presented in this thesis is an effort to develop a controller that will automatically control the amount of braking required in a commercial vehicle under all braking conditions. For the purpose of demonstration, this control scheme

has been implemented on our experimental setup at Texas A&M University. The results for a variety of test runs are illustrated in Chapter IV.

B. Outline of the Thesis

The following is a brief outline of the chapters that follow: Chapter II introduces a typical air brake system and identifies the function of all relevant components. Also, a description of the experimental setup at Texas A&M University is provided. In Chapter III, a scheme is derived to the control the pressure in the brake chamber. In Chapter IV, the control scheme is implemented on the experimental setup. The controller is corroborated for a variety of desired pressure trajectories in both full and partial brake applications. Chapter V presents concluding remarks and possible work for the future.

CHAPTER II

DESCRIPTION OF THE BRAKE SYSTEM AND EXPERIMENTAL SETUP

A. Air Brake System Description

A typical air brake system found in a commercial vehicle is comprised of a pneumatic subsystem and a mechanical subsystem. A detailed description of both follows:

1. Pneumatic Subsystem

A schematic of a typical pneumatic subsystem in air brakes can be seen in Figure 1. Air from the compressor is accumulated in storage reservoirs. When the driver applies the brake pedal, the primary and secondary circuit ports of the treadle valve are opened. The rear brakes are engaged when the air flowing in the primary circuit opens the relay valve, thus modulating the air that travels from the storage reservoirs into the rear brake chambers. The front brake chambers are actuated by the secondary circuit of the treadle valve through a quick release valve. When the brake pedal is released, the exhaust ports in the treadle valve are opened, allowing the air from the brake chambers to flow out into the atmosphere.
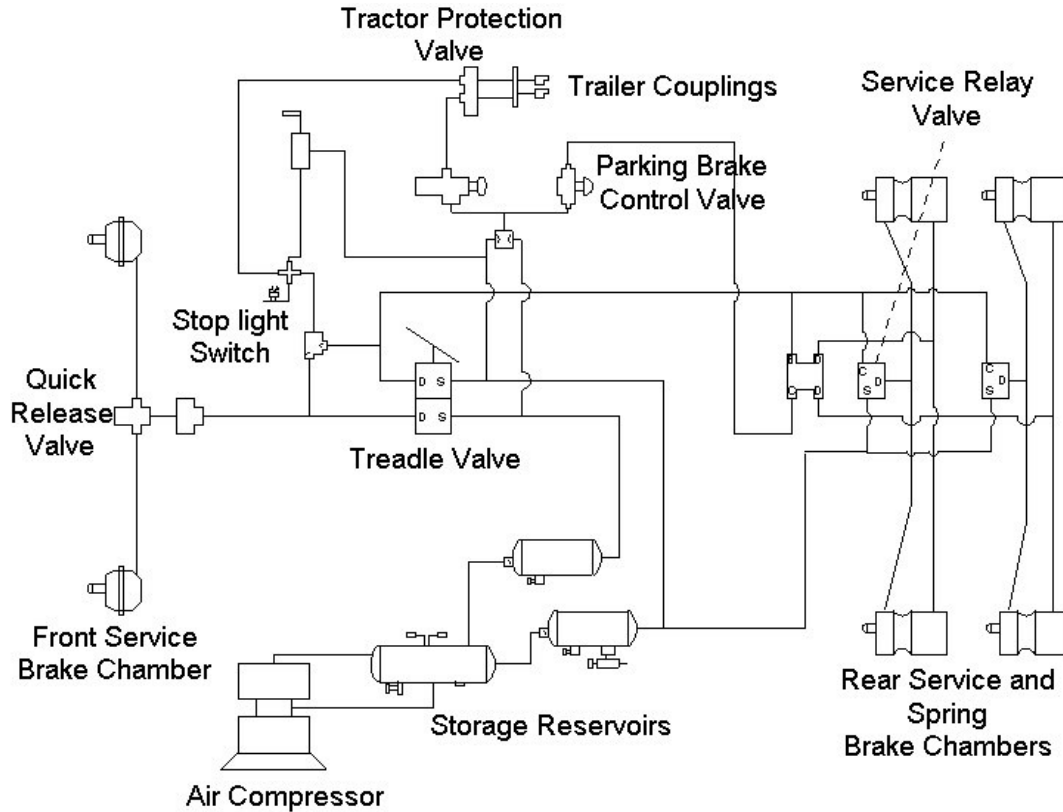
Figure 1 A general layout of the air brake system in trucks

2. Mechanical Subsystem

The S-cam foundation brake, found in around 85% of the commercial vehicles in United States [10], is illustrated in Figure 2. When the brake pedal is applied, air enters the brake chamber and acts on the diaphragm. The generated force results in the motion of the push rod, which in turn, rotates the S-cam through the slack adjuster. This rotation forces the brake shoes to make contact with the brake drum, thus retarding the wheel.
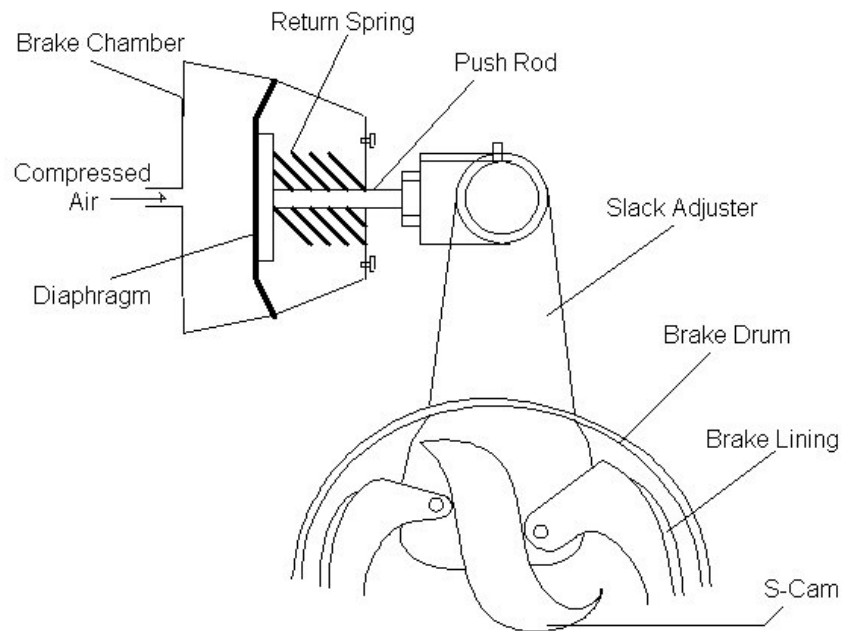
Figure 2 The mechanical subsystem of an S-cam air brake system

B. Experimental Setup Description

A schematic of the experimental setup is shown in Figure 3. The original setup that was used to generate the mathematical model included a storage reservoir, two "Type 20" front brake chambers, and a treadle valve. Recently the setup has been upgraded to include a second reservoir, two "Type 30" rear brake chambers, and relay and quick release valves. Furthermore, the original method of pneumatic actuation of the treadle valve has been upgraded to an electromechanical actuator, which allows for repeatable pedal actuation.

The actuator is the means for implementing the control scheme for the brake chamber pressure. The actuator shaft is interfaced with the motor through a timing belt drive and lead screw assembly. The details of the actuator are listed in Table 1 along with the specifications of the other mechanical components of the test bench. The actuator [15] has the following features: a brushless servo motor that allows for fast response and encoder/potentiometer feedback, a maximum thrust capacity of 3560 N (800 lbs), and a belt drive and ball screw assembly to minimize backlash. The entire system has been designed such that it can be installed with little modification to the previous setup.

A pressure transducer is mounted at the entrance of each of the four brake chambers by means of a custom designed and fabricated pitot tube fixture. A displacement transducer is mounted on each of the two front brake chamber push rods through appropriately fabricated fixtures in order to measure the push rod stroke. All the transducers are interfaced with a connector block through shielded cables. The connector block is connected to a PCI-MIO-16E-4 DAQ board [16] (mounted on a PCI slot inside a desktop computer) that collects the data during brake application and release. An application program is used to collect and store the data in the computer. The actuator is controlled by means of a B8501 servo drive. The B8501 module receives a command input of 0-10VDC from the DAQ analog output, which is interpreted as the range of minimum and maximum actuator stroke [17]-[19]. The B8501 receives position feedback from a displacement transducer that is installed inside the actuator. The specifications of these components can be seen in Table 2.
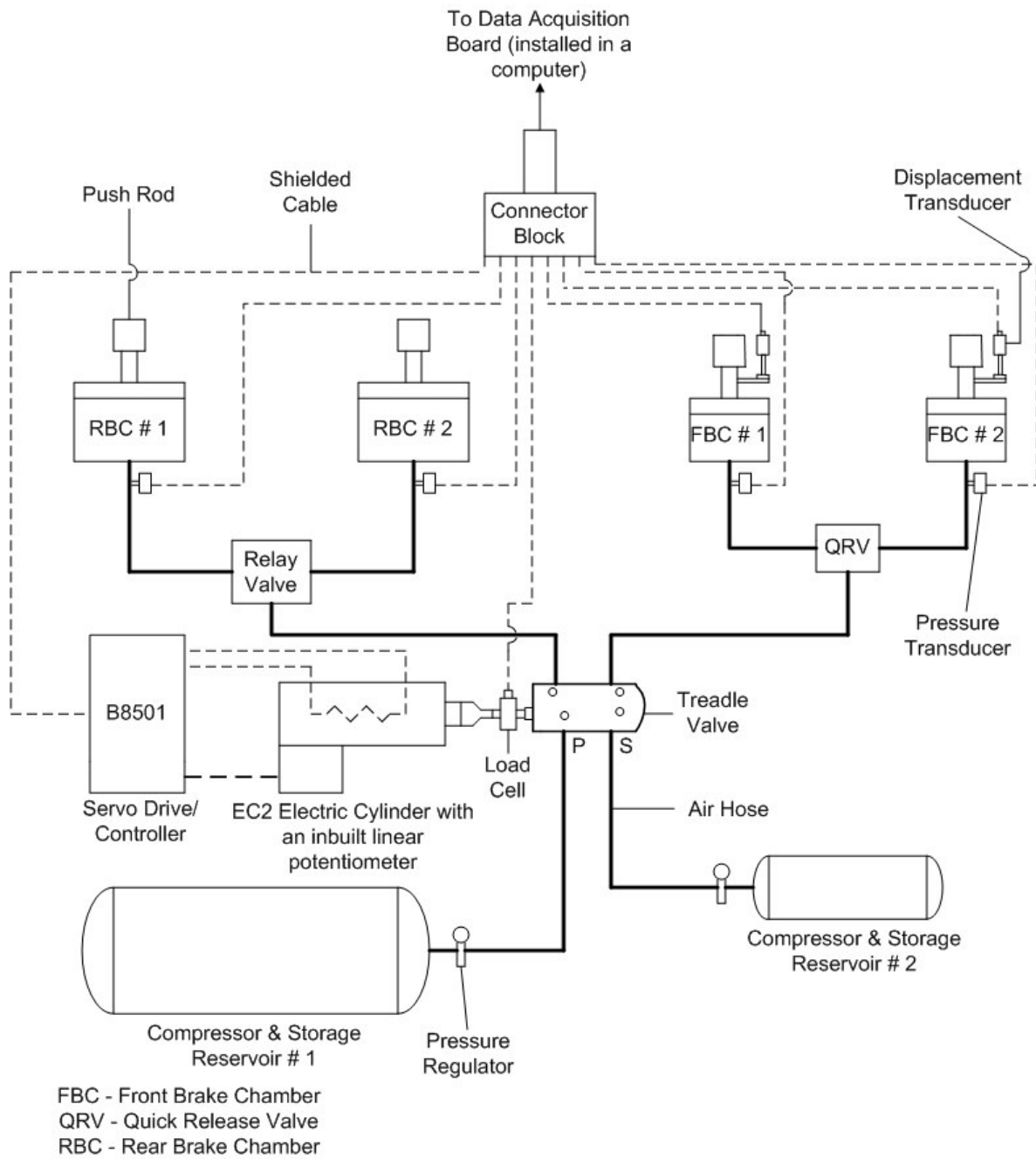
Figure 3 A schematic of the experimental setup

Table 1 Brake system components

Title	Manufacturer	Model Number	Description
Primary supply compressor	Campbell Hausfeld	WL651300AJ	The storage tank has a twelve gallon capacity.
Secondary supply compressor	Campbell Hausfeld	FP200200AV	The storage tank has a six gallon capacity.
Treadle valve	Bendix	E-7	Actuation exposes air in the storage tanks to the braking circuits.
Quick release valve	Bendix	QR1	Distributes air to the front brake chambers.
Relay valve	Bendix	R-12	Distributes air to the rear brake chambers.
Hoses	McMaster-Carr	Various sizes	Supply lines that run between all components of the system.
Front break chambers	Bendix	"Type 20"	Convert air pressure into a concentrated force for braking.
Rear brake chambers	Bendix	"Type 30"	Convert air pressure into a concentrated force for braking.
Pressure regulator	Omega	PRG501-120	Maintains a constant desired pressure for the air flowing into the treadle valve.

Table 2 Electrical system components

Title	Manufacturer	Model Number	Description
Electro-mechanical actuator	IDC	B23-2005B-100-MS1/MS6E MT1E-L	Provides position control of 0-100mm.
Actuator controller	IDC	B8501	Controls IDC actuator based on 0-10VDC input
Load cell	Omega	LC203-1K	Force range of up to 1000 lb force.
Load cell power source	Omega	DMD-465WB	Provides 10VDC excitation voltage.
Pressure transducers	Omega	PX181-100G5V	Pressure range of 0 to 100 psig.
Pressure transducer power source	Omega	U24Y101	Provides 24VDC power supply.
DAQ board	National Instruments	PCI-MIO-16E-4	16 analog inputs and 2 analog output channels.

The controller is implemented in a fashion as indicated by the block diagram in Figure 4. MathWorks'® Simulink® was used to write the code for the control scheme and interface it with the DAQ board to collect data during experiments. The numerical scheme written for the controller calculates the necessary value of desired plunger displacement (x_p) at each instant of time corresponding to the desired value of the brake chamber pressure and the actual pressure measurement at that instant of time. Then, this value of x_p is provided to the servo drive that moves the treadle valve plunger to the corresponding position through the electromechanical actuator.
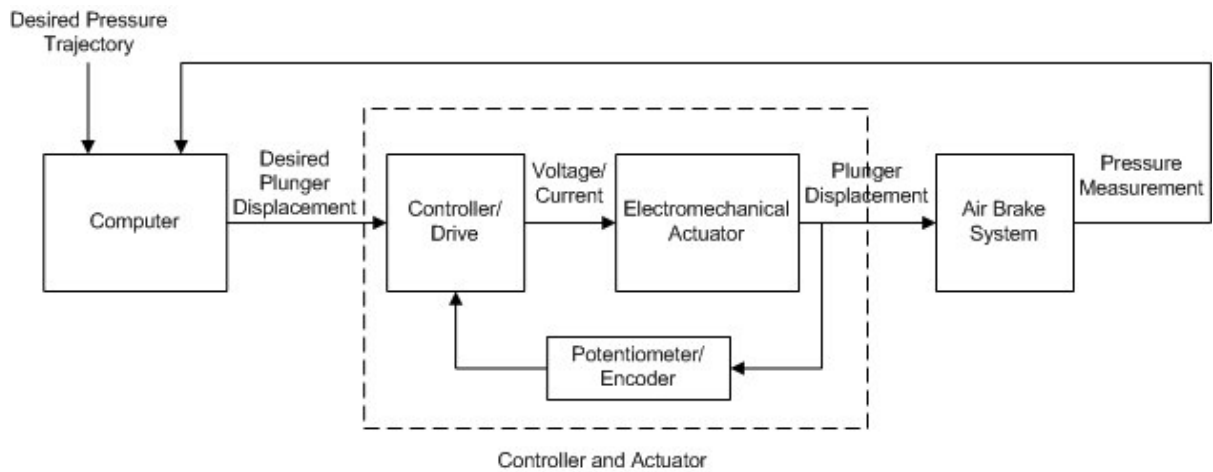

Figure 4 A block diagram of the pressure control scheme

CHAPTER III

CONTROLLER DEVELOPMENT

The controller has been developed based on the mathematical model of the treadle valve derived in [14]. For the sake of completeness, this model is provided in this chapter following a discussion of how it works. A cross-sectional view of the treadle valve with all assumed variable names can be seen in Figure 5. The brake foot pedal is normally connected to the treadle valve plunger. However, for our experimentation, the foot pedal has been replaced with an actuator. The treadle valve plunger displacement (x_p) is the variable that is modulated by the actuator.

The relationship between the plunger displacement and the pressure in the brake chamber is neither linear, nor is it continuous. The treadle valve functions in the following way: the force applied on the plunger is transmitted to the primary piston through the rubber graduating spring and the stem spring. Note that the force-deflection curve of the rubber graduating spring is nonlinear. When the displacement of the primary piston (x_{pp}) is equal to the constant distance of x_{pt}, it comes in contact with the primary valve assembly. Once the displacement of the primary valve assembly gasket (x_{pv}) is greater than zero, the primary inlet port opens and air flows from the reservoir to the brake chamber. This is referred to as the "apply phase". When the delivery pressure increases to a level where it balances the pedal input force, the primary inlet valve is closed with the primary exhaust

also remaining closed. This is the "hold phase". When the driver disengages the brakes, the return springs force all of the components back to their original positions. This action opens the exhaust port and the air in the brake chamber is exhausted to the atmosphere. This is denoted as the "exhaust phase". The controller developed in this thesis takes into account these phases of operation and the nonlinear response of the rubber graduating spring.
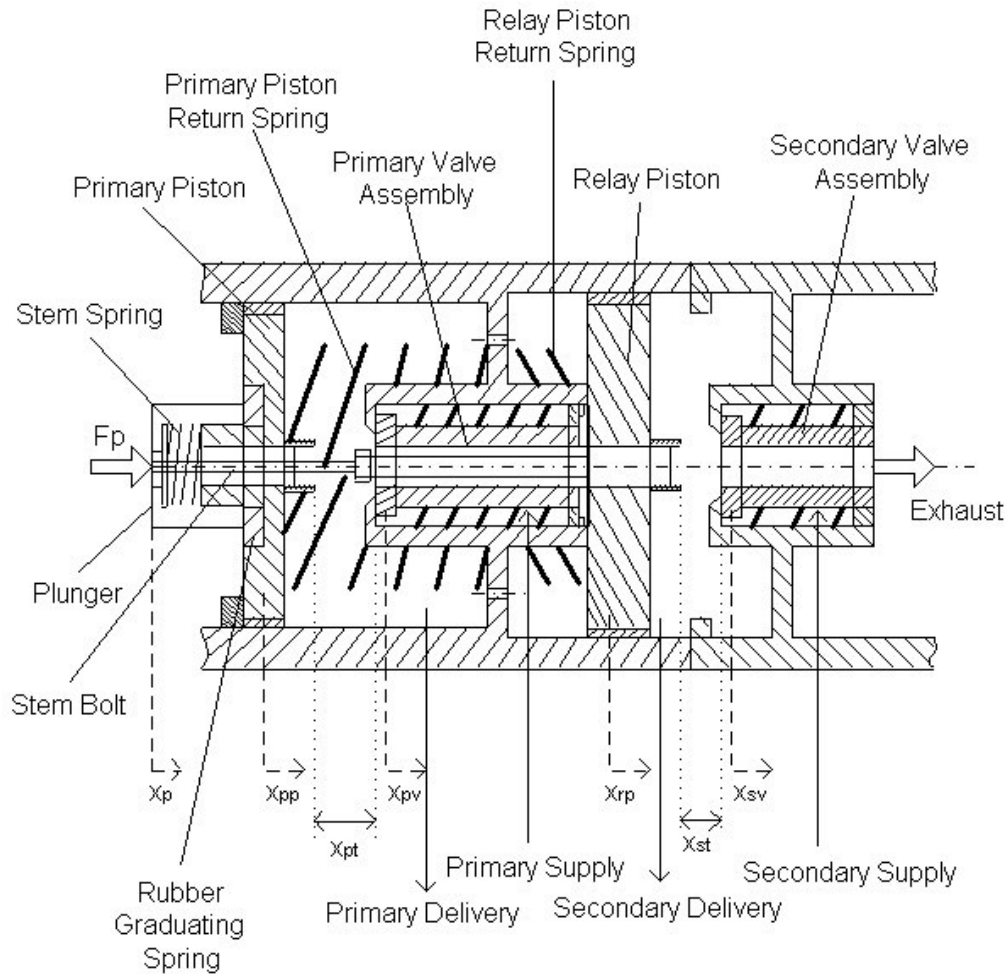

Figure 5 Cross-sectional view of the treadle valve

A. Model of the Treadle Valve

A lumped parameter model of the treadle valve has been developed and presented in [14]. In this section, a summary of the governing equations of this model is presented. The treadle valve opening has been modeled as a nozzle. The friction at the sliding surfaces of the treadle valve is assumed to be negligible since they are well lubricated. The springs in the treadle valve were tested and found to be linear in the region of their operation (except the rubber graduating spring). The governing equation of the primary piston during the apply and hold phases of the brake application process is given by

$$(M_{pp} + M_{pv})\left(\frac{d^2 x_{pp}(t)}{dt^2}\right) + K_2 x_{pp}(t) = K_{ss} x_p(t) + F_{gs} + F_1 - (A_{pp}$$
$$- A_{pv})P_{pd}(t) - P_{ps} A_{pv1} + P_{atm} A_{pp}, \tag{1}$$

and

$$F_1 = K_{pv} x_{pt} + F_{kssi} - F_{kppi} - F_{kpvi}, \tag{2}$$

$$K_2 = K_{ss} + K_{pp} + K_{pv}, \tag{3}$$

where M_{pp} is the mass of the primary piston, M_{pv} is the mass of the primary valve assembly gasket, K_{ss} is the stem spring constant, K_{pv} is the primary valve assembly return spring constant, K_{pp} is the primary piston return spring constant, F_{gs} is the force transmitted by the rubber graduating spring, F_{kssi} is the initial pre-load on the stem spring, F_{kppi} is the initial pre-load on the primary piston return spring, F_{kpvi} is the initial pre-load on the primary valve assembly return spring, A_{pp} is the net area of the primary piston exposed to the

delivered pressurized air, A_{pv} is the net cross-sectional area of the primary valve assembly gasket exposed to the pressurized air at the delivery, A_{pv1} is the net cross-sectional area of the primary valve assembly gasket exposed to the pressurized air at the supply, P_{pd} is the pressure of the primary delivery air at any instant of time, P_{ps} is the supply air pressure to the primary circuit, and P_{atm} is the atmospheric pressure.

As stated previously, the mechanical response (the load-deflection curve) of the rubber graduating spring is nonlinear. It has been tested to obtain the calibration curve illustrated in Figure 6. The deflection of the rubber graduating spring is denoted by x_{pd}.
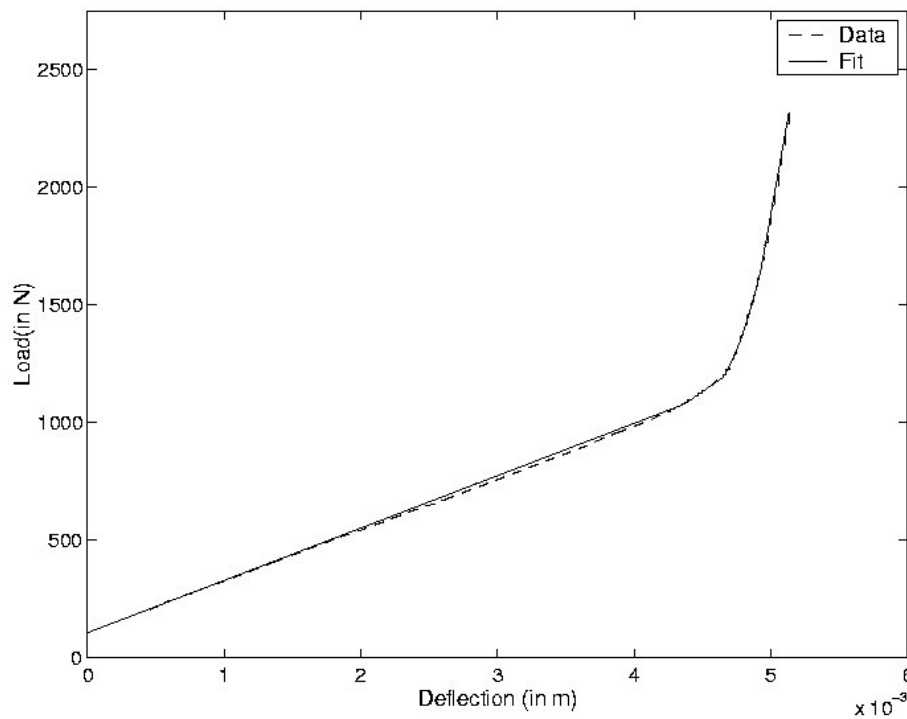

Figure 6   Calibration curve of the rubber graduating spring

The following relationship has been obtained from this curve:

$$F_{gs}(t) = \begin{cases} m_1 x_{pd}(t) + b_1 & \text{if } x_{pd}(t) \le r_1 \\ m_2 x_{pd}(t) + b_2 & \text{if } r_1 < x_{pd}(t) \le r_2 \\ a_1 x_{pd}^2(t) + a_2 x_{pd}(t) + a_3 & \text{if } r_2 < x_{pd}(t) \le r_3 \\ m_4 x_{pd}(t) + b_4 & \text{if } x_{pd}(t) > r_3 \end{cases} \qquad (4)$$

where

$$x_{pd}(t) = x_p(t) - x_{pp}(t) \qquad (5)$$

and the calibration constants have been determined from Figure 7.

The mass of the primary piston was found out to be around 0.16 kg and the magnitude of the spring and pressure forces was found to be in the order of 10^2 N. Thus, the acceleration required for the inertial forces to be comparable with the spring force and the pressure force terms has to be in the order of 10^2-10^3 m/s^2, which is not possible in this case. With this simplification, Equation (1) becomes

$$K_2 x_{pp}(t) = K_{ss} x_p(t) + F_{gs}(t) + F_1 - (A_{pp} - A_{pv})P_{pd}(t) - P_{ps}A_{pv1} + P_{atm}A_{pp}. \qquad (6)$$

The governing equation of motion of the primary piston during the exhaust phase can be derived in a similar manner to be

$$M_{pp}\left(\frac{d^2 x_{pp}(t)}{dt^2}\right) = F_{gs} + F_{kssi} + K_{ss}x_p(t) - (K_{ss} + K_{pp})x_{pp}(t) \\ - A_{pp}P_{pd}(t) + A_{pp}P_{atm} - K_{pp}x_{pp} - F_{kppi} \qquad (7)$$

Again neglecting inertia, Equation (7) is rewritten as

$$K_3 x_{pp}(t) = K_{ss} x_p(t) + F_{gs}(t) + F_2 - A_{pp} P_{pd}(t) + P_{atm} A_{pp},$$ (8)

where

$$F_2 = F_{kssi} - F_{kppi},$$ (9)

$$K_3 = K_{ss} + K_{pp}.$$ (10)

The above model will be used to control a single brake chamber connected to the primary circuit of the treadle valve. A simplified depiction of the interaction between the supply tank, treadle valve, and brake chamber can be seen in Figure 7. This identifies the variables P_o and P_b as the supply tank pressure and the brake chamber pressure respectively. The supply pressure to the treadle valve is maintained as a constant value of pressure through means of a pressure regulator.
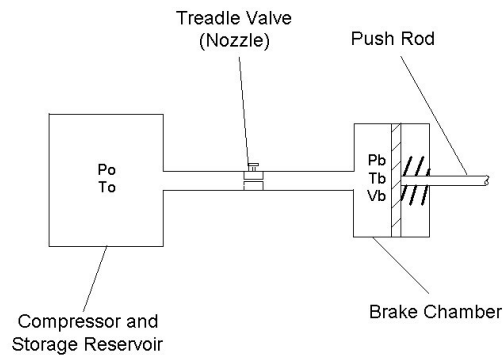

Figure 7 Simplified diagram of pneumatic subsystem to be controlled

It should be noted when the primary delivery port is connected directly to a front brake chamber, the term P_{pd} in the model is taken to be the same as P_b and the term P_{ps} is taken to be P_o.

B. Control Scheme Derivation

For the purpose of deriving the controller, the following relationship for the pressure transients in the brake chamber is assumed:

$$\dot{P}_b(t) = \lambda A_p(t), \tag{11}$$

where A_p is the cross-sectional area of the valve opening and λ is a positive constant whose value was determined experimentally. The goal of the controller is to reduce the error (e) between the desired pressure ($P_{b,des}$) and the measured pressure ($P_{b,meas}$) given by

$$e(t) = P_{b,meas}(t) - P_{b,des}(t). \tag{12}$$

Thus,

$$\dot{e}(t) = \dot{P}_{b,meas}(t) - \dot{P}_{b,des}(t). \tag{13}$$

Assume the following equation such that the error decays asymptotically to zero:

$$\dot{e}(t) = -Ce(t), \tag{14}$$

where C is a positive constant. Equations (12)-(14) can be combined and rewritten as

$$\dot{P}_{b,meas}(t) = \dot{P}_{b,des}(t) - C\left[P_{b,meas}(t) - P_{b,des}(t)\right]. \tag{15}$$

Combining this with Equation (11), the desired area of the valve opening is given by

$$A_p(t) = \frac{1}{\lambda}\left\{\dot{P}_{b,des}(t) - C\left[P_{b,meas}(t) - P_{b,des}(t)\right]\right\}. \tag{16}$$

Let us now derive the relationship between A_p and x_{pp}. During the apply phase

$$A_p(t) = \begin{cases} 2\pi\, r_{pv}[x_{pp}(t) - x_{pt}] & \text{during the apply phase} \\ 2\pi\, r_{pp}[x_{pt} - x_{pp}(t)] & \text{during the exhaust phase} \end{cases} \tag{17}$$

where r_{pv} is the external radius of the primary valve assembly inlet section and r_{pp} is the external radius of the primary piston exhaust seat.

The equations presented in the previous section provide the relationship between A_p and x_{pp} for the apply, hold, and exhaust phases of the brake application. The numerical scheme written for the controller solves the equations at each instant of time to calculate the necessary value of x_p corresponding to the values of $P_{b,des}$ and $P_{b,meas}$ at that instant of time. Then, this value of x_p is provided to the servo drive that moves the treadle valve plunger to the corresponding position through the electromechanical actuator. The numerical values for the parameters discussed in this chapter are presented in Table 3.

Table 3 Values of the parameters used in the controller calculations

Parameter	Value	Parameter	Value
A_{pv}	0.0003645 m^2	A_{pp}	0.002371 m^2
A_{pv1}	0.0002026 m^2	P_{atm}	101.356 kPa
K_{ss}	2846.545 N/m	F_1	-152.868 N
K_2	9832.181 N/m	F_2	-105.8624
K_3	7775.944 N/m	r_{pv}	0.01283 m
x_{pt}	0.002286 m	r_{pp}	0.01232 m
m_1	222831.478 N/m	b_1	104.9995 N
m_2	404767.9763 N/m	b_2	-689.8448 N
m_4	3264026.266 N/m	b_4	14433.1506 N
a_1	2736268733 N/m^2	r_1	0.004369 m
a_2	-966886378.6 N/m	r_2	0.004648 m
a_3	56227.168 N	r_3	0.004928 m
λ	5x10^8 Pa/(sm^2)		

CHAPTER IV

IMPLEMENTATION OF THE CONTROLLER

The control scheme presented in the previous section has been implemented in our experimental setup for the following variety of test runs carried out at different supply pressures:

    a). steps trajectories to the supply pressure and intermediate values to simulate emergency brake applications, (found on pages 26 through 28)

    b). ramp trajectories to the supply pressure and intermediate values to simulate normal brake applications (found on pages 29 through 32), and

    c). trapezoidal pulse trajectories with an amplitude equal to the supply pressure and intermediate values at a frequency of 0.1 Hz (found on pages 33 through 35).

One of the issues relating to the response of the brake system is illustrated in Figure 8. This figure is a plot of measured steady state values of the brake chamber pressure and the treadle valve plunger displacement for test runs carried out at a supply pressure of 722 kPa (90 psig). It can be seen that the majority of the pressure range is achieved within a span of 0.002 m of the treadle valve plunger displacement. The control scheme developed in Chapter III tackles this issue by using the model of the treadle valve. As a result, it will be seen shortly that the control scheme is able to track the pressure during partial applications in a reliable manner.
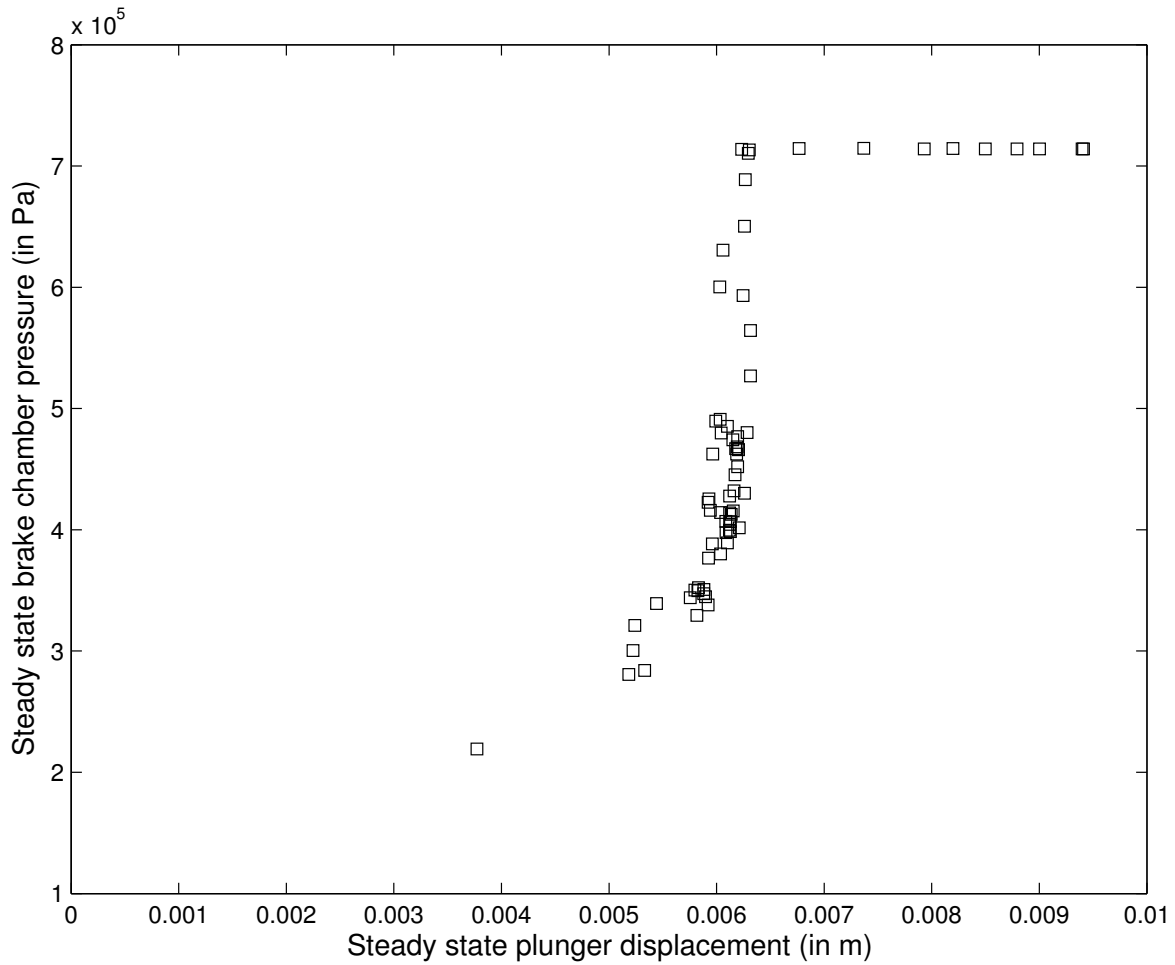
Figure 8 Steady state brake chamber pressure and treadle valve displacement at 722 kPa (90 psig)

supply pressure

The controller parameter (*C*) was adjusted during the implementation procedure to study its influence on the performance of the control scheme. In all the figures presented in this section, the dotted line indicates the desired brake chamber pressure trajectory. The response of the controller (measured brake chamber pressure) for three values of *C* = { 0.75, 1.25 and 1.75}, has been plotted for each case. In Figure 9, it can be observed that the

controller is able to track well the full step to the supply pressure of 515 kPa (60 psig) for all the three values of C. In the case of a partial step application to a steady state pressure of 377 kPa (40 psig) (see Figure 10), it is noted that the response of the controller becomes faster as the value of C is increased but the overshoot increases with it. Note that at $C = 1.75$ the steady state response becomes oscillatory in nature as the controller becomes very sensitive to small errors between the desired and the measured pressure. This behavior is not reflected in the full application (Figure 9) since the maximum steady state pressure that can be reached in any brake application is the supply pressure. Also, a time delay is noticed between the desired and the measured pressure at the initial stages of the pressure rise in these figures which is a result of the inherent nature of the response of the brake system. When the pressure error (e) starts to increase from zero, the controller begins to modulate the actuator resulting in the motion of the treadle valve plunger. But the treadle valve plunger has to first travel a distance equal to x_{pt} to close the exhaust port and then further motion is possible only after the pre-loads on the primary valve assembly gasket are overcome. After these pre-loads are overcome, the primary inlet port is opened and air starts to flow into the brake chamber. This behavior of the brake system is the cause of the time delay that is observed in these figures. Figures 11-14 demonstrate the same step input tests for supply pressures of 584 kPa (70 psig) and 653 kPa (80 psig).
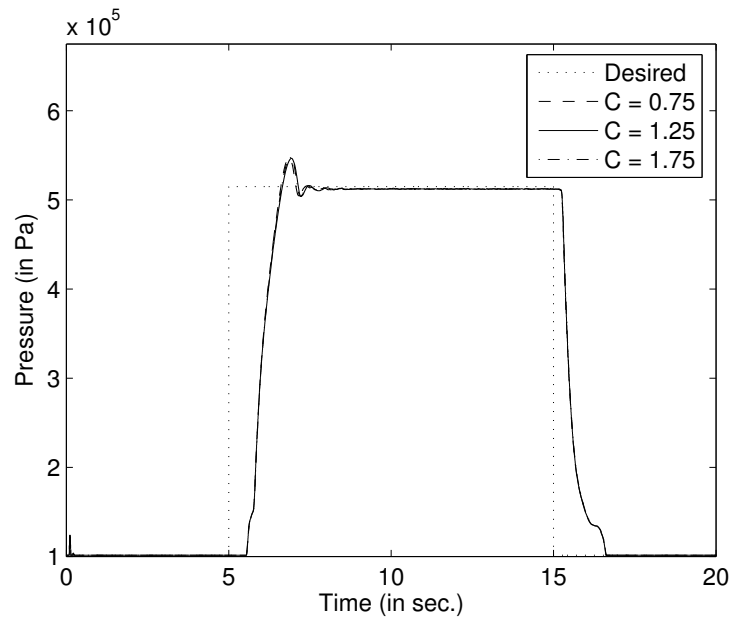
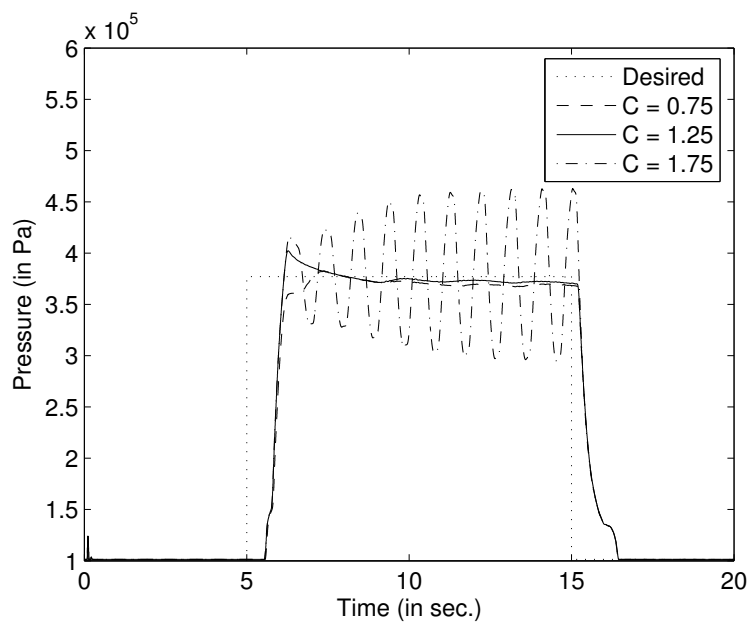**Figure 9 Controller response for a full step to the 515 kPa (60 psig) supply**

Figure 10 Controller response for a partial step to 377 kPa (40 psig) at 515 kPa (60 psig) supply
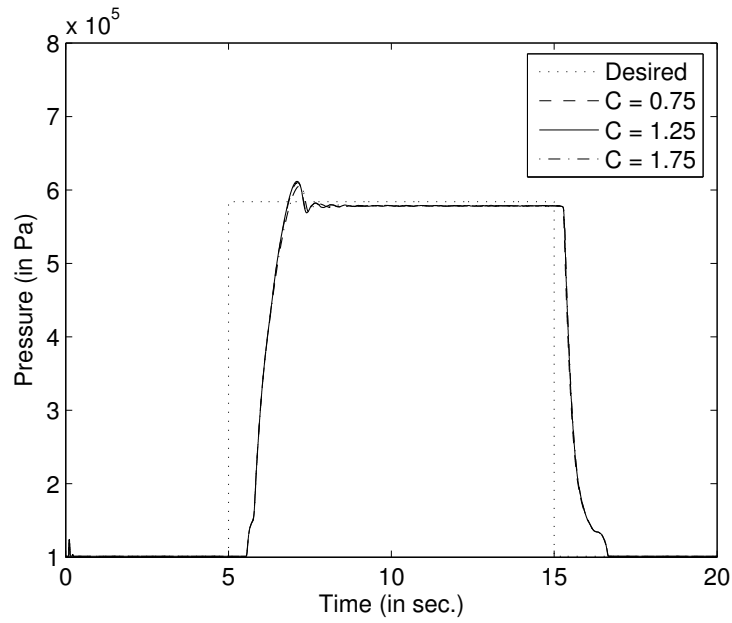
Figure 11 Controller response for a full step to the 584 kPa (70 psig) supply
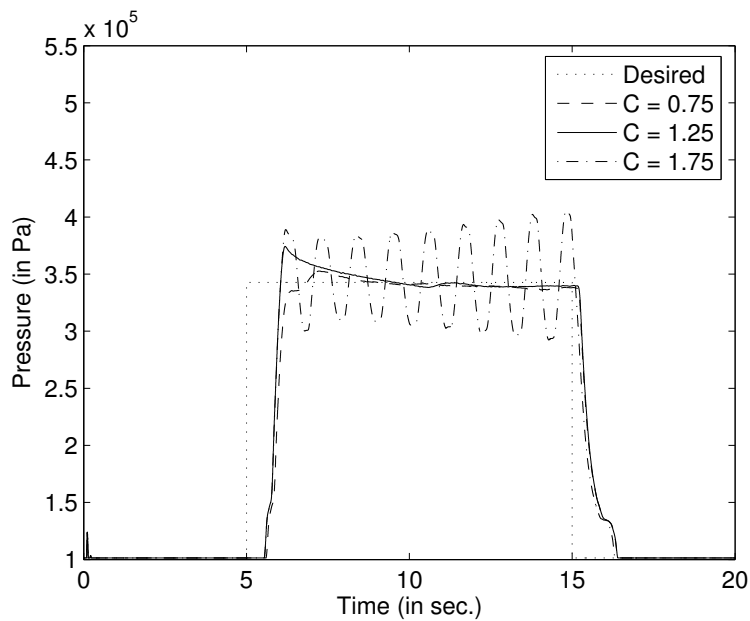

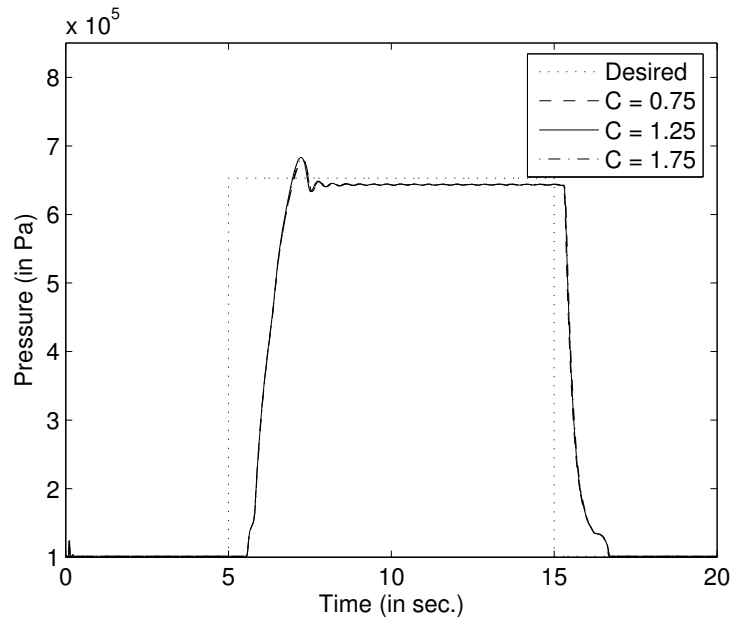**Figure 12 Controller response for a partial step to 343 kPa (35 psig) at 584 kPa (70 psig) supply**

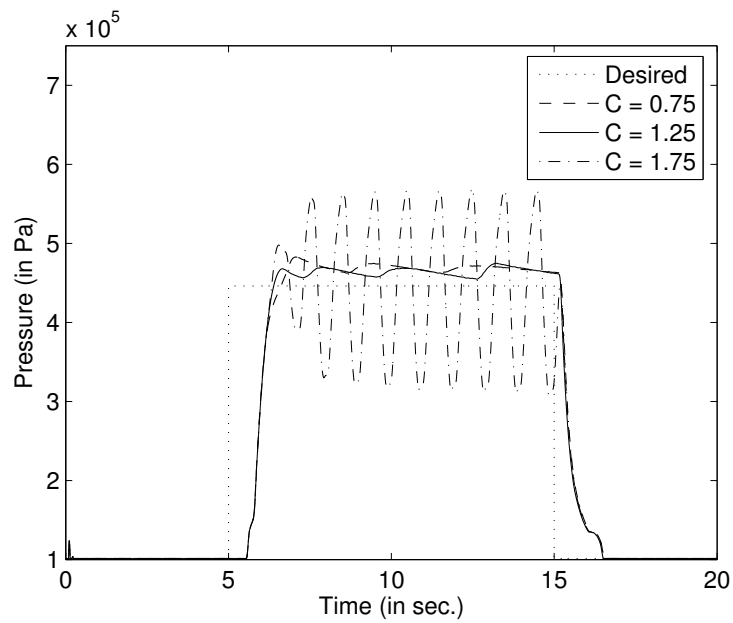**Figure 13 Controller response for a full step to the 653 kPa (80 psig) supply**

Figure 14 Controller response for a partial step to 446 kPa (50 psig) at 653 kPa (80 psig) supply

The response of the controller to a full ramp application to a steady state pressure of 515 kPa (60 psig) at a supply pressure of 515 kPa (60 psig) can be seen in Figure 15. Also, the controller response to a partial ramp application to a steady state pressure of 377 kPa (40 psig) at the same supply pressure can be seen in Figure 16. Once again, it can be observed that the steady state response becomes oscillatory when $C = 1.75$ during the partial brake application. Figures 17-20 demonstrate the same ramp trajectory input tests for supply pressures of 584 kPa (70 psig) and 653 kPa (80 psig).
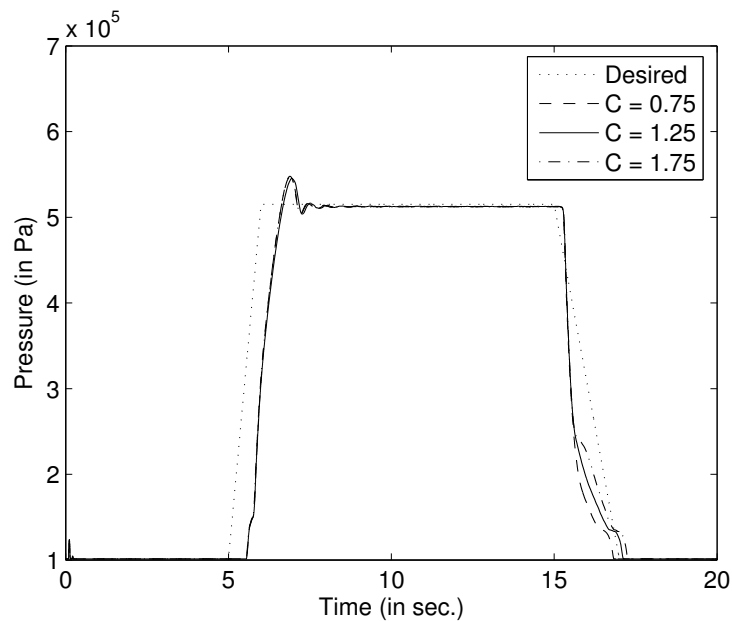

Figure 15 Controller response for a full ramp to the 515 kPa (60 psig) supply
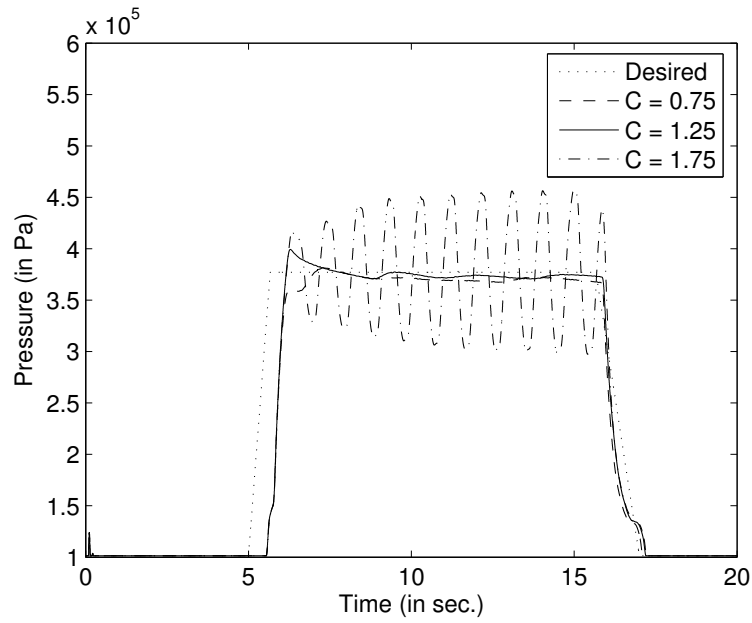
Figure 16 Controller response for a partial ramp to 377 kPa (40 psig) at 515 kPa (60 psig) supply
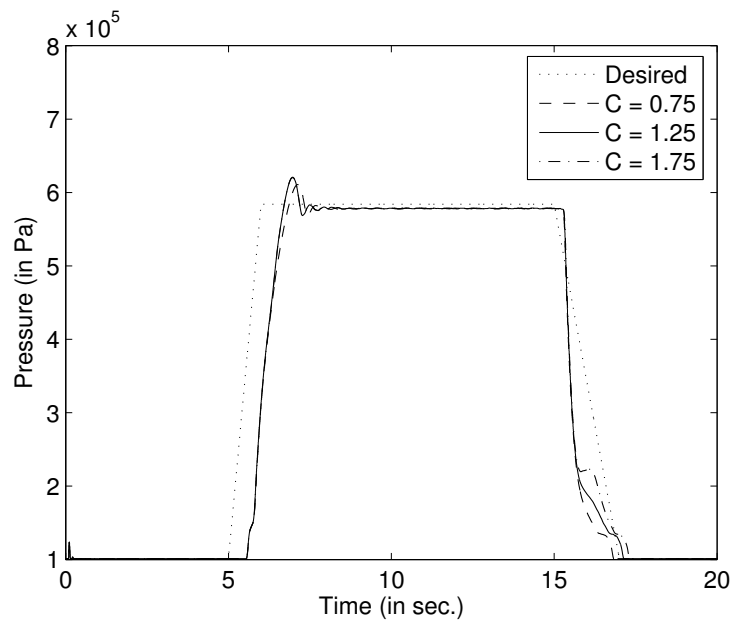

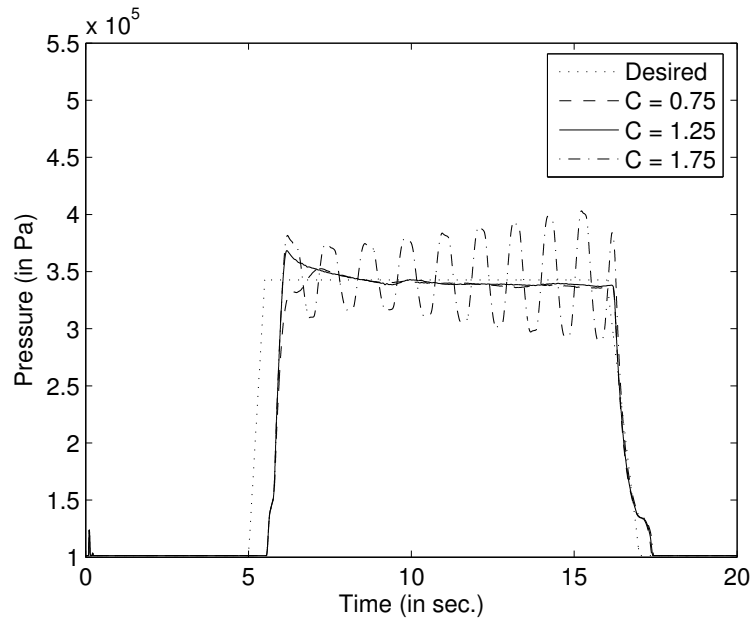**Figure 17 Controller response for a full ramp to the 584 kPa (70 psig) supply**

Figure 18 Controller response for a partial ramp to 342 kPa (35 psig) at 584 kPa (70 psig) supply
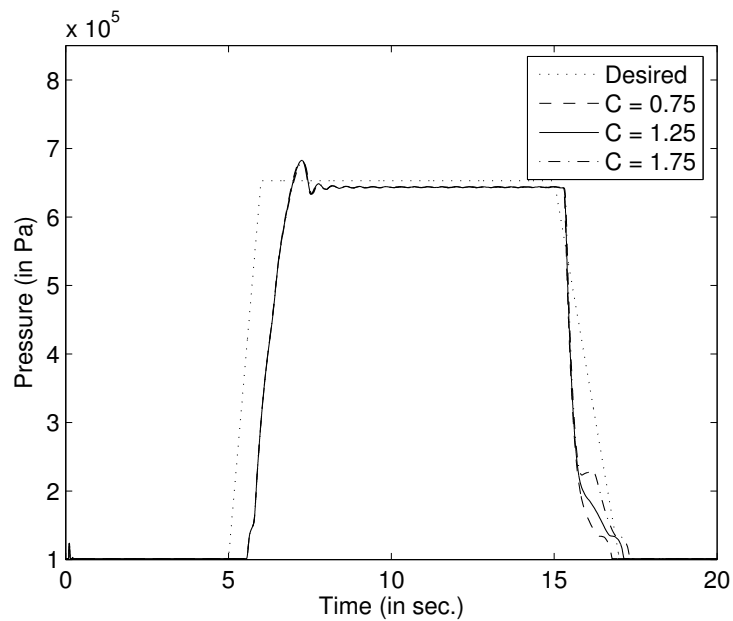

Figure 19 Controller response for a full ramp input to the 653 kPa (80 psig) supply
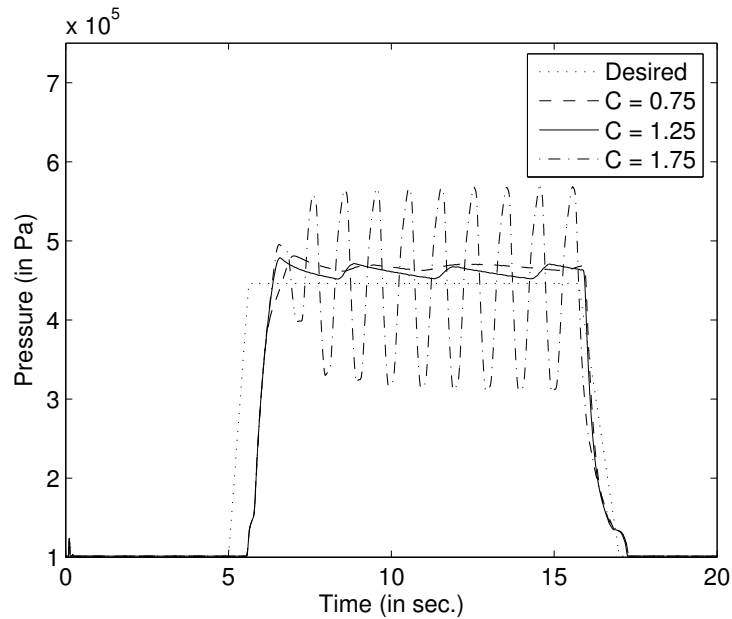
Figure 20 Controller response for a partial ramp to 446 kPa (50 psig) at 653 kPa (80 psig) supply

Figures 21 and 22 illustrate the performance of the controller to full and partial trapezoidal pulse trajectories at a supply pressure of 515 kPa (60 psig). The pulse trajectory chosen has a frequency of 0.1 Hz, i.e., one complete cycle of brake apply to the desired steady state pressure and the subsequent exhaust is completed in 10 seconds. Observe from these figures that the controller is able to track the desired pressure trajectories for repeated applications. Figures 23-26 demonstrate the same trapezoidal pulse trajectory input tests for supply pressures of 584 kPa (70 psig) and 653 kPa (80 psig).
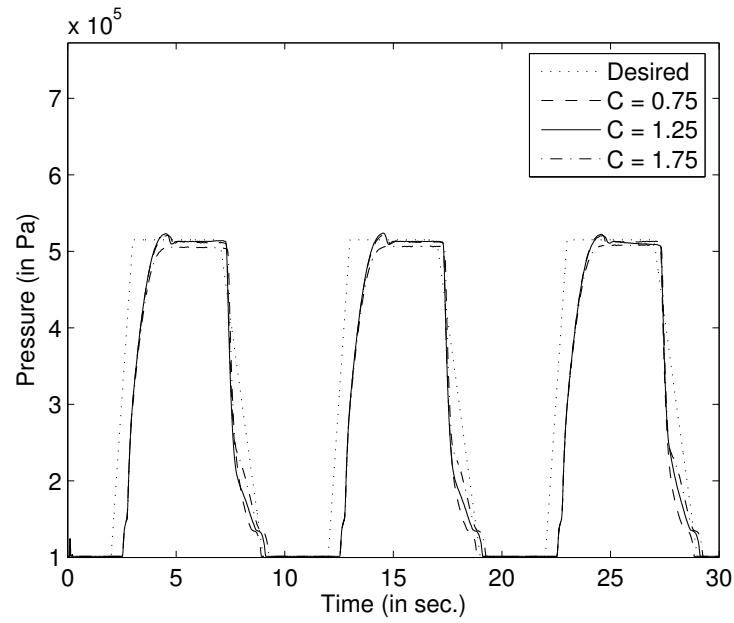
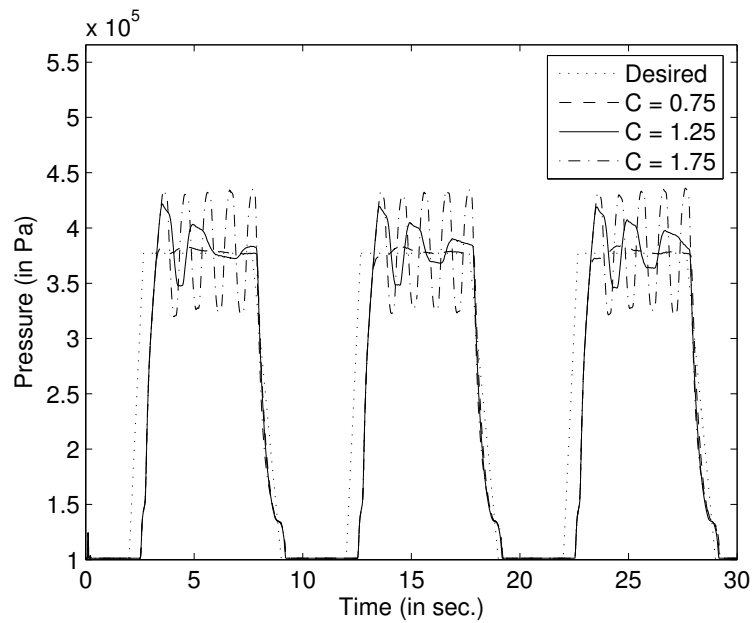**Figure 21 Controller response for a trapezoidal pulse to the 515 kPa (60 psig) supply**

Figure 22 Controller response for a trapezoidal pulse to 377 kPa (40 psig) at 515 kPa (60 psig) supply
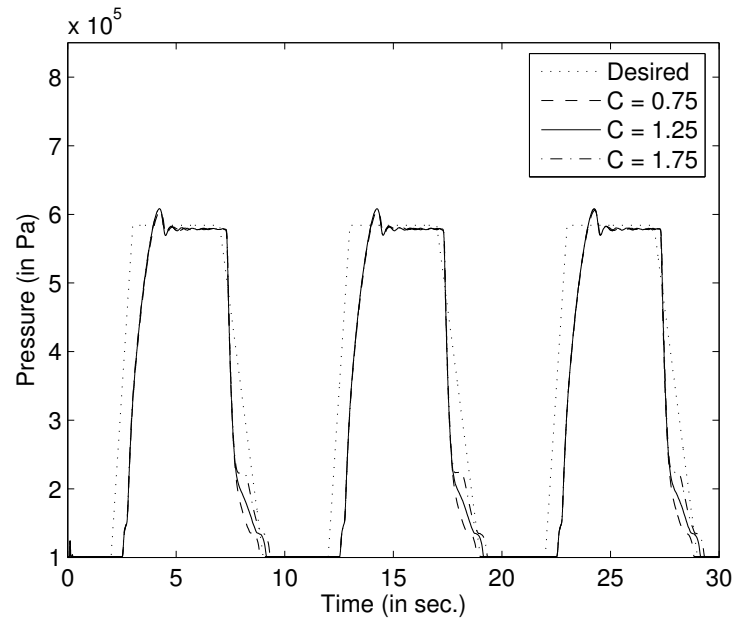
Figure 23 Controller response for a trapezoidal pulse to the 584 kPa (70 psig) supply
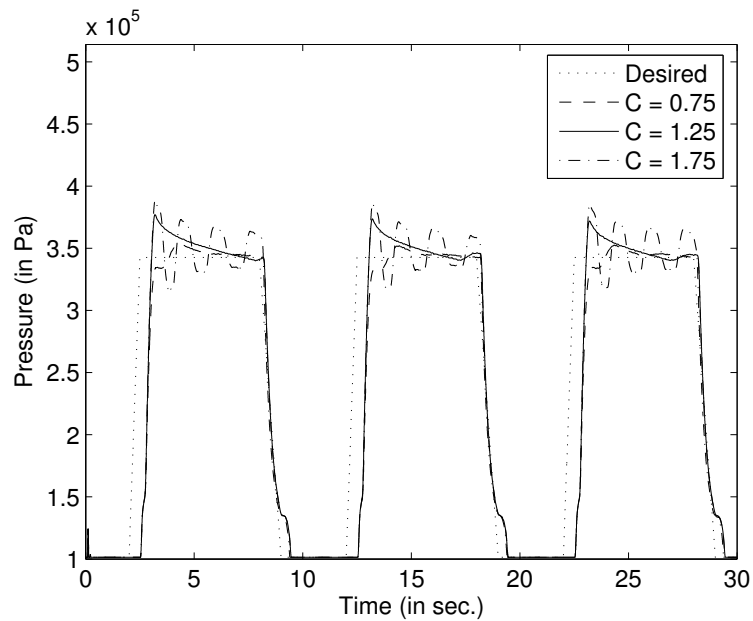

Figure 24 Controller response for a trapezoidal pulse to 342 kPa (35 psig) at 84 kPa (70 psig) supply
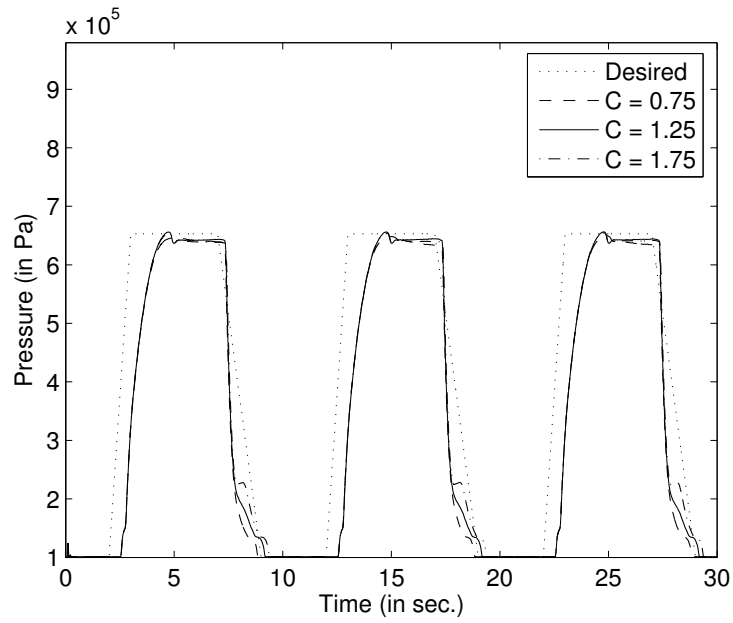
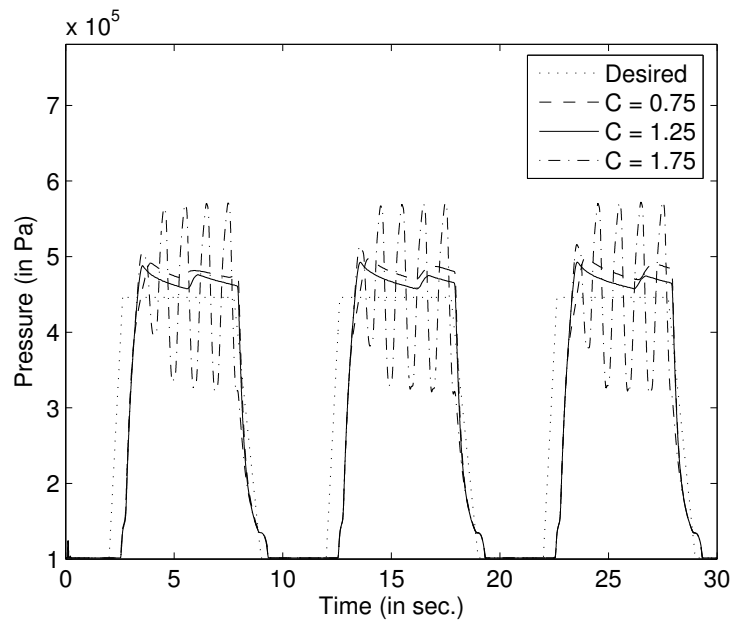**Figure 25 Controller response for a trapezoidal pulse to the 653 kPa (80 psig) supply**

Figure 26 Controller response for a trapezoidal pulse to 446 kPa (50 psig) at 653 kPa (80 psig) supply

CHAPTER V

CONCLUSIONS AND FUTURE WORK

In this thesis, a scheme has been presented for controlling the pressure in the brake chamber of the air brake system found in commercial vehicles. This scheme is based on the model of the treadle valve and it has been shown that such an approach has proved beneficial in tracking the pressure during partial brake applications. The efficacy of the scheme has been demonstrated by implementing it on our experimental setup for a variety of test runs. The responses due to various values of the controller gain parameter (C) have been compared. This scheme can be used for controlling the response of air brake systems as part of emerging technologies such as ACC systems for commercial vehicles.

Possible activities that can be carried out in the future include:

- expanding the control to the entire brake system, including all the front and rear brake chambers, and

- implementing a PID controller based on a time delay model [20], [21] of the brake system to study an alternative control scheme.

REFERENCES

[1]   S. J. Sobolak, "Simulation of the Ford vehicle speed control system," SAE, Tech. Rep. 820777, 1982.

[2]   P. G. Blaney, "Improvements to cruise controls utilizing microprocessor technology," SAE, Tech. Rep. 830662, 1983.

[3]   G.F. Franklin, J.D. Powell, and A. Emami-Naeini, *Feedback Control of Dynamic Systems*, Fourth Edition, Upper Saddle River, New Jersey: Prentice Hall, 2002.

[4]   Y. Harada, H. Miyata, Y. Hayakawa, and S. Fujii, "Cruise control system using adaptive control theory," SAE, Tech. Rep. 931917, 1993.

[5]   A. Ishida, M. Takada, K. Narazaki, and O. Ito, "A self-tuning automotive cruise control system using the time delay controller," SAE, Tech. Rep. 920159, 1992.

[6]   D. Wuh, "Design and comparison of autonomous intelligent cruise control systems," SAE, Tech. Rep. 942405, 1994.

[7]   P. Francher, Z. Bareket, S. Bogard, C. MacAdam, and R. Ervin, "Tests characterizing performance of an adaptive cruise control system," SAE Tech. Rep. 970458, 1997.

[8]   B. Riley, G. Kuo, B. Schwartz, J. Zumberge, and K. Shipp, "Development of a controlled braking strategy for vehicle adaptive cruise control," SAE Tech. Rep. 2000-01-0109, 2000.

[9] D. Swaroop and K. R. Rajagopal, "Intelligent Cruise Control Systems and Traffic Flow Stability," *Transportation Research Journal*, vol. C., no.7, pp. 329-352, December 1999.

[10] S.F. Williams and R.R. Knipling, "Automatic slack adjusters for heavy vehicle air brake systems," Research Report DOT HS 807 724, Washington D.C.: National Highway Traffic Safety Administration, February 1991.

[11] Omega Corporation, "Precision pressure regulators" Retrieved August 21, 2005 from http://www.omega.com/ppt/pptsc.asp?ref=PRG101

[12] Knorr-Bremse Corporation, "Knorr-Bremse systems for commercial vehicles" Retrieved August 21, 2005 from http://www.knorr-bremsesfn.com/

[13] Bendix Corporation, "Bendix ABS-6 advanced with ESP®: A brake through innovation in electronic stability", Retrieved August 22, 2005 from http://www.bendix.com/abs6/

[14] S.C. Subramanian, D. Swaroop, and K.R. Rajagopal, "Modeling the pneumatic subsystem of an S-cam air brake system," *Journal of Dynamic Systems, Measurement, and Control*, ASME, vol. 126, pp. 36-46, March 2004.

[15] Industrial Devices Corporation, *EC Series Electric Cylinders User's Manual*, P/N CUS10050 Version 1.0, Rockford, Illinios: Industrial Devices Corporation.

[16] National Instruments, *PCI E Series Manual: Multifunction I/O Devices for PCI Bus Computers*, Austin, Texas: National Instruments Corporation, July 2002.

[17] Industrial Devices Corporation, *B8001 Brushless Servo Drive Operator's Manual*, P/N PCW-4679 Rev. 1.5, Rockford, Illinois: Industrial Devices Corporation, May 1998.

[18] Industrial Devices Corporation, *B8501 Brushless Analog Position Control Manual Supplement*, P/N PCW-4712 Rev. 1.01, Rockford, Illinois: Industrial Devices Corporation, June 1995.

[19] Industrial Devices Corporation, *IDC Servo Tuner Operator's Manual*, P/N PCW-4710 Rev. 1.00, Rockford, Illinois: Industrial Devices Corporation, April 1995.

[20] G.J. Silva, A. Datta, and S.P. Bhattacharyya, "Stabilization of Time Delay Systems," *Proceedings of 2000 American Control Conference*, June 2000, pp. 963-970.

[21] M.T. Ho, G.J. Silva, A. Datta, and S.P. Bhattacharyya, "Real and Complex Stabilization: Stability and Performance," *Proceedings of 2004 American Control Conference*, July 2004, pp.4126-4138.

VITA

Christopher Leland Bowlin was born in the city of Fort Worth, Texas. He was brought up in the cities of Watauga and North Richland Hills and received his diploma from Richland High School in May 2000. In May 2004, he obtained his Bachelor of Science in mechanical engineering from Texas A&M University – College Station. He joined the Mechanical Engineering Department at Texas A&M University as a graduate student in June, 2004, and graduated with his Master of Science in mechanical engineering in December, 2005. Christopher may be contacted through Dr. Darbha Swaroop at the Department of Mechanical Engineering, Texas A&M University, College Station, TX 77843-3123.